Solar and Stellar Magnetic Fields: Origins and Manifestations
Proceedings IAU Symposium No. 354, 2019
A. Kosovichev, K. Strassmeier & M. Jardine, ed.
doi:10.1017/S1743921319009864

Magnetic field and prominences of the young, solar-like, ultra-rapid rotator AP 149

Tianqi Cang, Pascal Petit, Colin Folsom and Jean-Francois Donati

Institut de Recherche en Astrophysique et Planétologie, Université de Toulouse, CNRS, CNES, 31400 Toulouse, France

Abstract. Young solar analogs reaching the main sequence experience very strong magnetic activity, directly linked to their angular momentum loss through wind and mass ejections. We investigate here the surface and chromospheric activity of the ultra-rapid rotator AP 149 in the young open cluster alpha Persei. With a time-series of spectropolarimetric observations gathered over two nights with ESPaDOnS, we are able to reconstruct the surface distribution of brightness and magnetic field using the Zeeman-Doppler-Imaging (ZDI) method. Using the same data set, we also map the spatial distribution of prominences through tomography of H-alpha emission. We find that AP 149 shows a strong cool spot and magnetic field closed to the polar cap. This star is the first example of a solar-type star to have its magnetic field and prominences mapped together, which will help to explore the respective role of wind and prominences in the angular momentum evolution of the most active stars.

Keywords. stars: individual: AP 149, stars: magnetic field, stars: solar-type, stars: rotation, stars: spots, stars: winds

1. Introduction

Magnetic activity of solar-type stars is an important ingredient in their early evolutionary phases. Young Suns tend to have high rotation rates since they have conserved most of the angular momentum acquired during the stellar formation process, and this rapid rotation plays a key role in their evolution (see the review of Bouvier 2013). High rotation rates are responsible for the efficient amplification of internal magnetic fields, through the action of global stellar dynamos.

Tomographic mapping is a powerful tool to characterize the surface magnetic field of rapid rotators. Since its first application to HR 1099 (Donati *et al.* 1992), this approach has been applied to several dozens of cool active stars on the main sequence (Folsom *et al.* 2018). Early investigations dedicated to young Suns (e.g. Donati *et al.* 2003, Petit *et al.* 2008) provide unique information about magnetic geometries and differential rotation probing a range of stellar parameters (mass, age, rotation age).

Prominences are among the most spectacular manifestations of stellar magnetic activity. For rapidly rotating stars, prominence systems become much more massive and extended than on the Sun (see review by Collier Cameron 1999). Prominences and stellar winds remove the angular momentum of stars and become a critical contributor to the early evolution of active stars.

In a first step towards the exploration of the magnetic field and prominences of ultra-rapidly rotating young suns, we investigated the G type star AP 149 (also named V530 Per), which is a young member of the α Persei open cluster.

Table 1. Parameters of AP 149

Parameter	Value	Ref.	Parameter	Value	Ref.
Distance	167.7 ± 15 pc	1,2	Mass	$1.03 \pm 0.13\ M_{\odot}$	1
Age	33^{+10}_{-7} Myr	1	$log\ L_x$	31.2	5
$T_{\rm eff}$	5281 ± 96 K	1	Rossby number	0.0128 ± 0.0019	1
log g	4.1 ± 0.19	1	Co-rotation radius	$1.92\ R_*$	1
$[Fe/H]$	0	1	$v\ sini$	$105.6\ {\rm km\,s^{-1}}$	1
m_V^{max}	11.657 ± 0.13	4	Eq. rot. period	0.3205 ± 0.0002 d	1
m_K	9.422 ± 0.019	4	$d\Omega$	$0.043 \pm 0.007\ {\rm rad\,d^{-1}}$	1
m_J	10.08 ± 0.019	4	Inclination angle	$35 \pm 0.2^{\circ}$	1
Luminosity	$0.76 \pm 0.18\ L_{\odot}$	1	Radial velocity	$-0.96 \pm 0.04\ {\rm km\,s^{-1}}$	1
Radius	$1.04 \pm 0.11\ R_{\odot}$	1			

References: 1. This work 2. Yen *et al.* (2018) 3. Stauffer *et al.* (1999) 4. Zacharias *et al.* (2012) 5. Pillitteri *et al.* (2013).

2. Observations

We obtained a time-series of spectropolarimetric observations of AP 149 in late 2006 (29 Nov and 05 Dec). The data were collected by the ESPaDOnS spectropolarimeter (Donati *et al.* 2006a), mounted at the Canada-France-Hawaii Telescope (CFHT). The observation was optimized to have full coverage of the rotational phase and normalized, reduced 56 Stokes I, and 14 Stokes V spectra are extracted. The LSD method (Donati *et al.* 1997) is used to combine a list of selected spectral lines to produce a pseudo line profile with improved S/N.

3. Fundamental Parameters

By combining literature measurements and ZDI results, we derive fundamental parameters of AP 149 and locate it on the H-R diagram. Details of the parameters are shown in Table 1.

4. Brightness imaging

By applying the Doppler Imaging method (DI, Vogt *et al.* 1987) using the ZDI code of Folsom *et al.* (2018), we recovered the surface brightness distribution of AP 149 in Fig 1. The reconstruction includes a solar-like differential rotation law, with a roughly solar shear level optimizing our model.

5. Magnetic field

Zeeman Doppler Imaging technique (ZDI, Semel 1989; Donati *et al.* 2006b; Folsom *et al.* 2018) is applied to model the two nights of Stokes V data, in order to reconstruct the 2D magnetic field distribution of AP 149. The map of the three components is shown in Fig.1. According to the map, the average surface magnetic field is 150G, with local peaks slightly above 1kG. About 2/3 of the magnetic energy belongs to the toroidal field component. Moreover, the complexity of the magnetic field is very high, with only 1.1% of the magnetic energy stored in the dipolar component.

6. Differential Rotation

The very dense phase coverage of our time-series constitutes a very good basis for studying the short term evolution of photospheric brightness, especially under the action of differential rotation. In our model, the rotation rate Ω is assumed to vary with the latitude (θ), following a simple surface dependence: $\Omega(\theta) = \Omega_{eq} - d\Omega \sin^2\theta$. A χ^2 minimizing method is used to derive the differential rotation $d\Omega$ and the rotational rate of the equator Ω_{eq} (Petit et al. 2002), shown in Figure 3. The quantitative results can be found in Table 1, and highlight a shear level roughly solar in magnitude.

https://doi.org/10.1017/S1743921319009864 Published online by Cambridge University Press

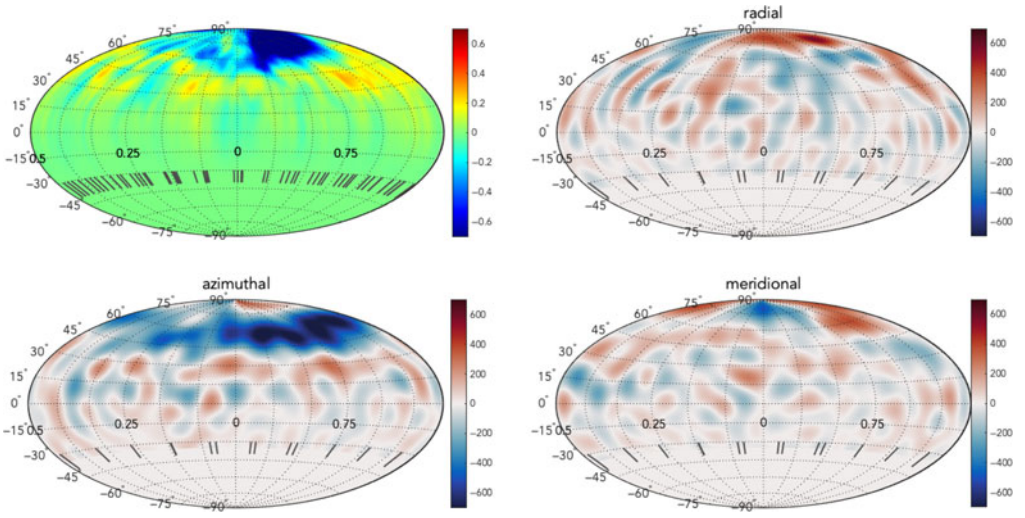

Figure 1. Brightness and Magnetic Map of AP 149. Logarithmic normalized brightness map (upper left) of AP 149 reconstructed assuming a combination of dark (blue) and bright (yellow) spots. A large, dark spot is identified close to the pole, as well as a complex spot distribution at lower latitudes. Since the inclination is small, most of the southern hemisphere could not be observed and modeled. The other three panels show different field components in a spherical projection with the unit in Gauss. For the radial (upper right) and meridional (lower right) components, the strongest magnetic spots are found close to the pole. For the azimuthal (lower left) component, a ring of negative field is reconstructed above a latitude of 45°.

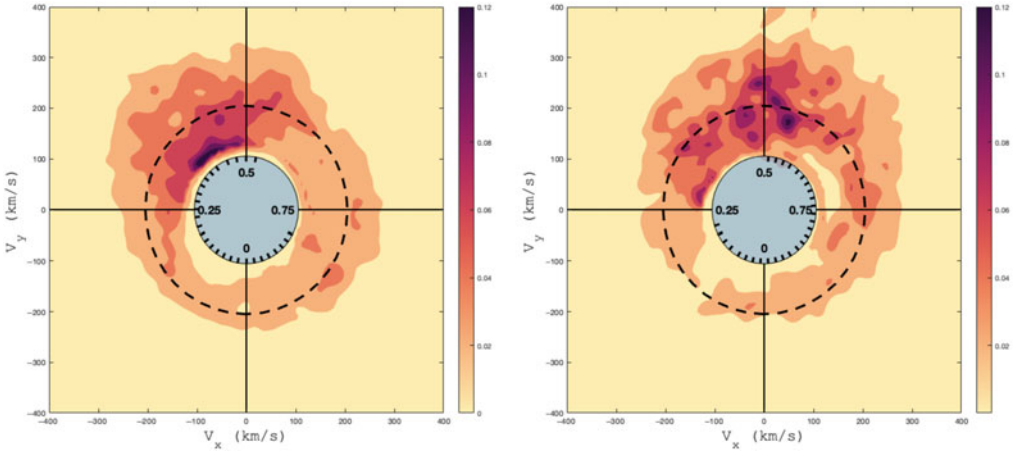

Figure 2. Dynamic Spectra showing the $H\alpha$ line of AP 149. The upper and lower panels are for 29 Nov and 05 Dec, respectively. From left to right, we display the observations, the outcome of the tomographic model, and the residuals. $H\alpha$ mapping from the first night leads to a reduced $\chi^2 = 6.8$, while the second night provides us with a reduced $\chi^2 = 7.5$.

7. Prominence System

For active stars, prominences are constituted of cool, dense gas trapped in closed magnetic loops, which always be connected with stellar wind. The prominence structure produces strong, rotationally-modulated, double peak $H\alpha$ emission. The line profiles of $H\alpha$ are always seen in emission throughout the observing sequence of AP 149, and we

https://doi.org/10.1017/S1743921319009864 Published online by Cambridge University Press

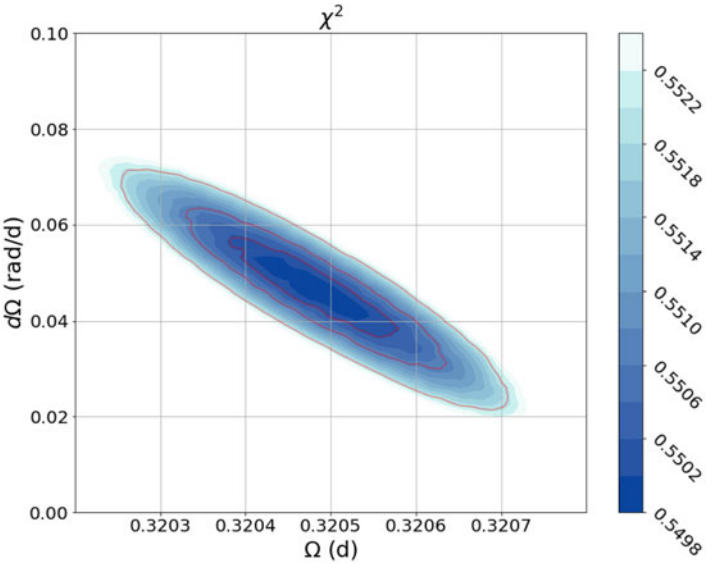

Figure 3. Reduced χ^2 map for the shear parameter $d\Omega$ and the equatorial rotation rate $\Omega_{\rm eq}$. The three red solid lines illustrate the 1σ, 2σ, and 3σ confidence intervals.

reconstructed prominence maps of AP 149 for the two observational nights (see Fig. 2), unveiling clues of short-term variations.

References

Bouvier, J. 2013, EAS Publications Series, 143
Collier Cameron, A. 1999, Solar and Stellar Activity: Similarities and Differences, 146
Donati, J.-F., Brown, S. F., Semel, M., *et al.* 1992, *A&A*, 265, 682
Donati, J.-F., Semel, M., Carter, B. D., *et al.* 1997, *MNRAS*, 291, 658
Donati, J.-F., Collier Cameron, A., & Petit, P. 2003, *MNRAS*, 345, 1187
Donati, J.-F., Catala, C., Landstreet, J. D., *et al.* 2006a, Solar Polarization 4, 362a
Donati, J.-F., Howarth, I. D., Jardine, M. M., *et al.* 2006b, *MNRAS*, 370, 629
Folsom, C. P., Bouvier, J., Petit, P., *et al.* 2018, *MNRAS*, 474, 4956
Folsom, C. P., Petit, P., Bouvier, J., *et al.* 2016, *MNRAS*, 457, 580
Lodieu, N., McCaughrean, M. J., Barrado Y Navascues, D., *et al.* 2005, VizieR Online Data Catalog, J/A+A/436/853
Petit, P., Donati, J.-F., & Collier Cameron, A. 2002, *MNRAS*, 334, 374
Petit, P., Dintrans, B., Solanki, S. K., *et al.* 2008, *MNRAS*, 388, 80
Pillitteri, I., Remage Evans, N., Wolk, S. J., *et al.* 2013, *AJ*, 145, 143
Semel, M. 1989, *A&A*, 225, 456
Stauffer, J. R., Barrado y Navascués, D., Bouvier, J., *et al.* 1999, *ApJ*, 527, 219
Vidotto, A. A., Gregory, S. G., Jardine, M., *et al.* 2014, *MNRAS*, 441, 2361
Vogt, S. S., Penrod, G. D., & Hatzes, A. P. 1987, *ApJ*, 321, 496
Yen, S. X., Reffert, S., Schilbach, E., *et al.* 2018, *A&A*, 615, A12
Zacharias, N., Finch, C. T., Girard, T. M., *et al.* 2012, VizieR Online Data Catalog, I/322A

https://doi.org/10.1017/S1743921319009864 Published online by Cambridge University Press